Theoretical investigation of the motional states of the nitrite ion in alkali halide crystals

G. K. Pandey, M. Massey, and K. L. Pandey
Physics Department, Allahabad University, Allahabad, India
(Received 26 July 1990)

A microscopic model for the substitutional NO_2^- impurity ion in NaCl-structure alkali halide crystals is developed on the basis of a specific theoretical potential. Coulomb, induction, and short-range interactions are included to obtain expressions for the barriers hindering the rotational motion of the impurity in the matrix cage. Preferred orientations, off-center displacements, and barrier parameters for this impurity are calculated in KCl, KBr, and KI host crystals. The results are used to explain most of the features of the infrared spectra in these impurity systems.

I. INTRODUCTION

Recently, much experimental and theoretical interest has been shown towards alkali halide crystals doped with molecular impurities. The comprehensive review articles by Narayanamurti and Pohl[1] and Frank Bridges[2] cover most of the experimental findings on the subject. The well-studied molecular impurities are OH^-, CN^-, NO_2^-, and SH^- ions along with their isotopically substituted species in different alkali halide crystals. The systems have been extensively studied by ultraviolet, infrared, and Raman spectroscopy and also by the measurements of various thermal properties such as specific heat, thermal conductivity, and paraelectric cooling, etc. A detailed understanding of these properties requires a knowledge of the various motional states of the impurity in the lattice vacancy. For the simpler cases of diatomic impurities, these states are now well understood in terms of specific models,[3-10] and the behavior of the impurity's stretching,[11] translational,[12] and angular motional states[13,14] for different lattices and different experimental conditions is also well understood. For the case of a polyatomic impurity, the situation is not so clear because of the complicated rotational degrees of freedom of the molecule. The polyatomic impurity that has been studied the most is the NO_2^- impurity in KCl, KBr, KI, NaCl, and NaBr crystals. For understanding the motional states of these impurity-lattice systems, many kinds of experiments have been performed. Sack and Moriaty[15] have measured the dielectric constant of these systems and have concluded that this impurity can rotate even at very low temperatures. They also concluded that in the KCl crystal the NO_2^- ion sits at the normal lattice site with a dipole moment 0.21 D. However, in the KI crystal, its center of mass is displaced by a distance, which increases its dipole moment in the crystal to 0.97 D. Narayanamurti *et al.*[1,16] performed detailed infrared and thermal-conductivity measurements on these systems. They also performed electric-field- and stress-field-induced dichroism experiments to ascertain the equilibrium orientational configuration of the impurity in the lattice vacancy. Their conclusions for the KCl case is that in this lattice the symmetry axis of the NO_2^- ion lies along either of the twelve $\langle 110 \rangle$ directions. They did not perform this kind of experiment for the KBr and KI crystals. Avarmaa and Rebane[17] analyzed the rotational structure of the pure electronic and zero-phonon lines in the vibronic spectra of these systems. They modified some of the methods of interpreting the experimental results in an empirical way and presented a better way of analyzing the orientational states of the impurity in the lattice vacancy. Earlier, Timusk and Staude,[18] Sievers and Lytle,[19] and Renk[20] carried out far-infrared spectroscopic studies of these systems and observed a multiplet of line structure, which reflected the complicated rotational and other kinds of motions of the impurity in these lattices. More recently, Shepherd, Evans, and Fitchen[21-23] carried out Raman and vibronic absorption spectra studies for the KCl, KBr, KI, and NaBr crystals doped with this impurity. They also carried out stress-induced dichroism and splitting measurements of the vibronic lines to determine more conclusively the equilibrium orientational configuration of the impurity in these crystals. Rebane *et al.*[24-26] used the Raman scattering (RS) technique to infer that in KCl, KBr, and RbCl, the motions around the B and C axes can be treated as small librations, while in KI, the molecule is frozen in its equilibrium orientations and performs only small librations around all the axes.

A clear understanding of the various experimental results requires a theoretical knowledge of the equilibrium orientational configuration of the impurity, the potential barrier hindering different kinds of angular motions and possible off-center-of-mass displacement of the impurity from the lattice. Attempts to explain or understand some of the motional states were made by Narayanamurti *et al.*,[16] Evans and Fitchen,[22] Avarmaa,[17] and others.[18-20,27] However, these attempts were empirical in nature and considered the potential barriers hindering angular motion of the impurity on a one-dimensional model. Also, they assumed certain minimum-energy orientational configurations of the impurities in the crystal, which was based upon experiments in some cases (e.g., KCl:NO_2^-) and on intuition on others (e.g., KBr:NO_2^- and KI:NO_2^-). No attempt to understand this minimum-energy orientational configuration of the impurity on the basis of a specific theoretical potential was done.

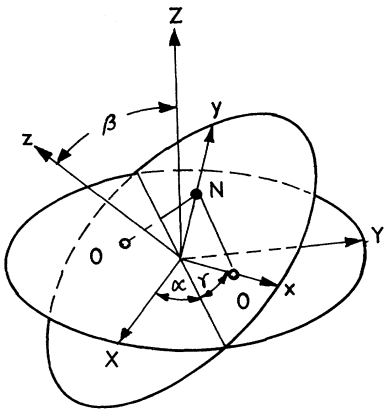

FIG. 1. Configuration of the impurity in the lattice and illustration of the space-fixed coordinate system (XYZ) and molecule-fixed coordinate system (xyz) connected through Eulerian angles α, β, and γ. The molecule-fixed axes x, y, and z are identified as the A, B, and C axes, respectively, of Ref. 2 (see Fig. 5 also). The solid circle shows a nitrogen atom and the hollow circles show oxygen atoms.

In this paper we have made an attempt to explain various experimental observations connected with NO_2^- impurity with the help of a model developed on the basis of a specific theoretical potential. The paper is organized as follows. In Sec. II, the form of the proper angle-dependent potential present at the site of the impurity in the lattice is discussed. Also, a relationship between the various possible minimum-energy orientational configurations of the impurity to the defined potential parameters is developed. In Sec. III, expressions for the defined potential parameters are obtained on the basis of first-principles calculations. In Sec. IV, an outline of the calculations of the potential parameters and the possible off-center displacement of the NO_2^- impurity in the KCl, KBr, and KI lattices is presented. In Sec. V, the results based on the present theoretical investigations are discussed. A summary and conclusions are given in Sec. VI.

II. THE CRYSTALLINE FIELD POTENTIAL AND MINIMUM-ENERGY ORIENTATIONAL CONFIGURATION OF THE IMPURITY

The form of the potential acting at the impurity site must be consistent with the octahedral symmetry of the crystal and the C_{2v} molecular symmetry of the nitrite ion. If α, β, and γ represent the three Eulerian angles describing the orientational coordinates of the impurity in the space-fixed coordinate system (XYZ) of the crystal (see Fig. 1), then the proper potential in which the impurity performs the angular motions can be expressed as

$$\begin{aligned} V_c = {} & K(0)[\cos^4\beta+\sin^4\beta(\sin^4\gamma+\cos^4\gamma)] \\ & +K(2)\{\cos2\alpha[(-1+8\cos^2\beta-7\cos^4\beta)+\cos4\gamma(1-\cos^4\beta)]+\sin2\alpha[\sin4\gamma(-\cos\beta+2\cos^3\beta)]\} \\ & +K(4)\{\cos4\alpha[(1-2\cos^2\beta+\cos^4\beta)+\tfrac{1}{7}\cos4\gamma(1+6\cos^2\beta+\cos^4\beta)]+\sin4\alpha[\tfrac{4}{7}\sin4\gamma(-\cos\beta-\cos^3\beta)]\} \ . \end{aligned} \tag{1}$$

Here, $K(0)$, $K(2)$, and $K(4)$ are the barrier parameters analogous to the Devonshire K parameter for the simpler diatomic impurities. This form of potential for triatomic impurities having C_{2v} symmetry has also been used by Sauer.[5] The barrier parameters $K(0)$, $K(2)$, and $K(4)$ used by Sauer are different from the corresponding parameters used in this paper. Flygare[28] has also used the above form of the potential expressed in terms of rotation matrices and barrier parameters $H(0)$, $H(2)$, and $H(4)$. However, the parameters used by Sauer or Flygare can be easily related to the barrier parameters used in this work.

Differentiating Eq. (1) partially with respect to α, β, and γ and setting them equal to zero, we get the conditions for extrema in the potential. One can easily put these extrema configurations into four groups. The minima configurations are as detailed below.

Group I,

$$\begin{aligned} &\alpha=0,\pm\pi/2,\pi \ , \\ &\beta=0,\pm\pi/2,\pi \ , \\ &\gamma=0,\pm\pi/2,\pi \ . \end{aligned} \tag{2}$$

This corresponds to the molecular configuration in the lattice in which the symmetry axis of the molecule lies along either of the six $\langle 001 \rangle$ directions and the line joining the two oxygen atoms along the corresponding $\langle 100 \rangle$ directions.

Group II,

$$\begin{aligned} &\alpha=0,\pm\pi/2,\pi \ , \\ &\beta=\pm\pi/2 \ , \\ &\gamma=\pm\pi/4,\pm3\pi/4 \ . \end{aligned} \tag{3}$$

This corresponds to the configuration in which the symmetry axis of the molecule lies along either of the twelve $\langle 110 \rangle$ directions and the O-O axis along the corresponding $\langle 1\bar{1}0 \rangle$ directions.

Group III,

$$\begin{aligned} &\alpha=0,\pm\pi/2,\pi \ , \\ &\beta=\pm\pi/4,\pm3\pi/4 \ , \\ &\gamma=0,\pm\pi/2,\pi \ . \end{aligned} \tag{4}$$

This corresponds to the molecular configuration in which the symmetry axis of the molecule lies along either of the six ⟨001⟩ directions and the O-O axis along the corresponding ⟨110⟩ directions.

Group IV,

$$\alpha=\pm\pi/4,\pm 3\pi/4\ ,$$
$$\beta=\pm\pi/2\ , \tag{5}$$
$$\gamma=0,\pm\pi/2,\pi\ .$$

This corresponds to the molecular configurations in which the symmetry axis of the molecule lies along either of the twelve ⟨110⟩ directions and the O-O axis along the corresponding ⟨001⟩ directions. These four molecular impurity orientations are suitably shown in Fig. 2.

The condition for minima to occur along a given group of equilibrium orientational configurations is that the Jacobian be positive and definite as well as $\partial^2 V_c/\partial\alpha^2$, $\partial^2 V_c/\partial\beta^2$, and $\partial^2 V_c/\partial\gamma^2$, i.e.,

$$\begin{vmatrix} \frac{\partial^2 V_c}{\partial\alpha^2} & \frac{\partial^2 V_c}{\partial\alpha\partial\beta} & \frac{\partial^2 V_c}{\partial\alpha\partial\gamma} \\ \frac{\partial^2 V_c}{\partial\beta\partial\alpha} & \frac{\partial^2 V_c}{\partial\beta^2} & \frac{\partial^2 V_c}{\partial\beta\partial\gamma} \\ \frac{\partial^2 V_c}{\partial\gamma\partial\alpha} & \frac{\partial^2 V_c}{\partial\gamma\partial\beta} & \frac{\partial^2 V_c}{\partial\gamma^2} \end{vmatrix} > 0 \tag{6}$$

and also

$$\frac{\partial^2 V_c}{\partial\alpha^2}>0;\ \frac{\partial^2 V_c}{\partial\beta^2}>0;\ \frac{\partial^2 V_c}{\partial\gamma^2}>0\ . \tag{7}$$

This gives the following conditions for minima to occur.

Group I,

$$\begin{aligned} &-4K(0)+16K(2)-(16/7)K(4)>0\ , \\ &-4K(0)-16K(2)-(16/7)K(4)>0\ , \\ &-(128/7)K(4)>0\ . \end{aligned} \tag{8}$$

Group II,

$$\begin{aligned} &-2K(0)+16K(2)-(40/7)K(4)>0\ , \\ &4K(0)+16K(2)+(16/7)K(4)>0\ , \\ &8K(2)-(96/7)K(4)>0\ . \end{aligned} \tag{9}$$

Group III,

$$\begin{aligned} &-2K(0)-4K(2)+(8/7)K(4)>0\ , \\ &-2K(0)+4K(2)+(8/7)K(4)>0\ , \\ &(128/7)K(4)>0\ . \end{aligned} \tag{10}$$

Group IV,

$$\begin{aligned} &-2K(0)-16K(2)-(40/7)K(4)>0\ , \\ &4K(0)-16K(2)+(16/7)K(4)>0\ , \\ &-8K(2)-(96/7)K(4)>0\ . \end{aligned} \tag{11}$$

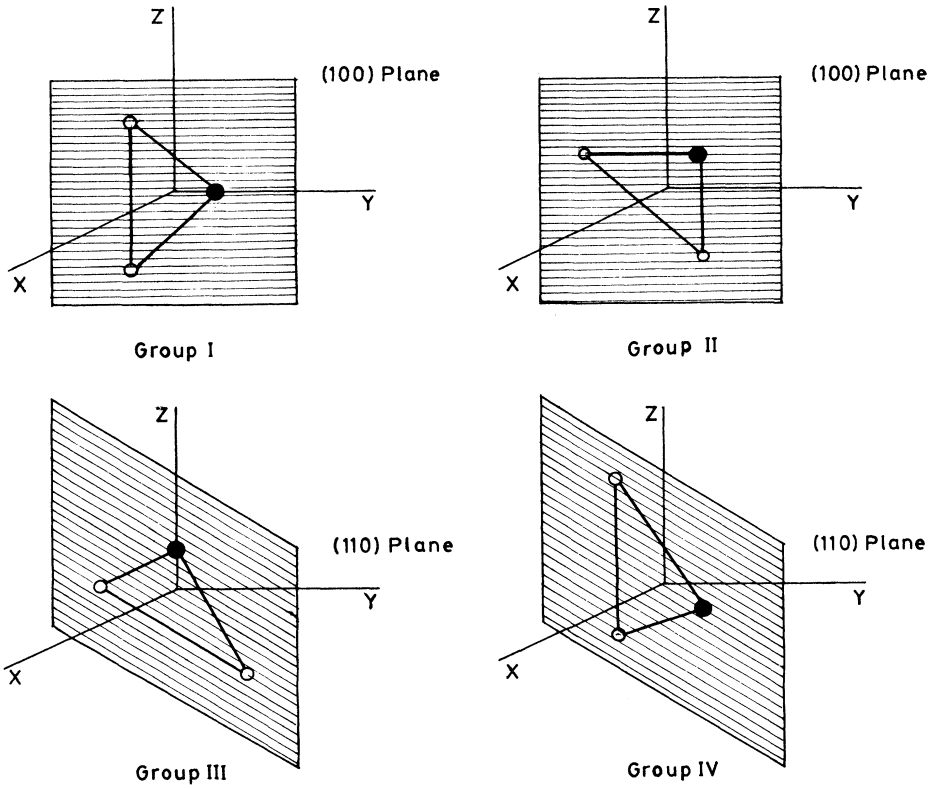

FIG. 2. The minimum-energy orientational configurations of NO_2^- in alkali halide crystals categorized in four groups as obtained from the theoretical considerations of the model potential at the impurity site.

Figures 3 and 4 show, respectively, the regions for the various potential minima in the $K(0)/K(4)$ and $K(2)/|K(4)|$ plane for positive and negative values of $K(4)$.

For $K(4)$ positive, the important points to note are as follows.

(i) No potential minima can occur along group-I directions.

(ii) There is a certain set of values for $K(0)/|K(4)|$ and $K(2)/|K(4)|$ for which no potential minima could occur in the lattice. This has been shown as a blank region in Fig. 3 and is given by

$$\begin{aligned} &-\frac{12}{7} < \frac{K(2)}{|K(4)|} < +\frac{12}{7}\,, \\ &\frac{5}{15} - \frac{1}{8}\frac{K(0)}{|K(4)|} < \frac{K(2)}{|K(4)|} < \frac{5}{14} + \frac{1}{8}\frac{K(0)}{|K(4)|}\,, \\ &\frac{8}{7} + \frac{1}{2}\frac{K(0)}{|K(4)|} < \frac{K(2)}{|K(4)|} < \frac{8}{7} - \frac{1}{2}\frac{K(0)}{|K(4)|}\,. \end{aligned} \tag{12}$$

(iii) For the following conditions, the potential minima could occur along group-II directions only:

$$\begin{aligned} &\frac{K(2)}{|K(4)|} > \frac{12}{7}\,, \\ &\frac{K(2)}{|K(4)|} > \frac{5}{14} + \frac{1}{8}\frac{K(0)}{|K(4)|}\,, \\ &\frac{K(2)}{|K(4)|} > \frac{8}{7} - \frac{1}{2}\frac{K(0)}{|K(4)|}\,. \end{aligned} \tag{13}$$

(iv) For

$$\begin{aligned} &\frac{K(2)}{|K(4)|} < -\frac{12}{7}\,, \\ &\frac{K(2)}{|K(4)} < -\frac{5}{14} - \frac{1}{8}\frac{K(0)}{|K(4)|}\,, \\ &\frac{K(2)}{|K(4)|} < -\frac{8}{7} + \frac{1}{2}\frac{K(0)}{|K(4)|}\,, \end{aligned} \tag{14}$$

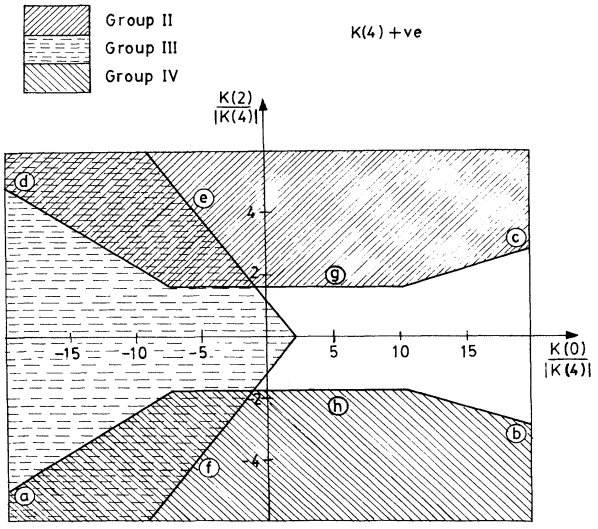

FIG. 3. The regions for the various potential minima in the $K(0)/|K(4)|$ and $K(2)/|K(4)|$ plane for a positive value of $K(4)$.

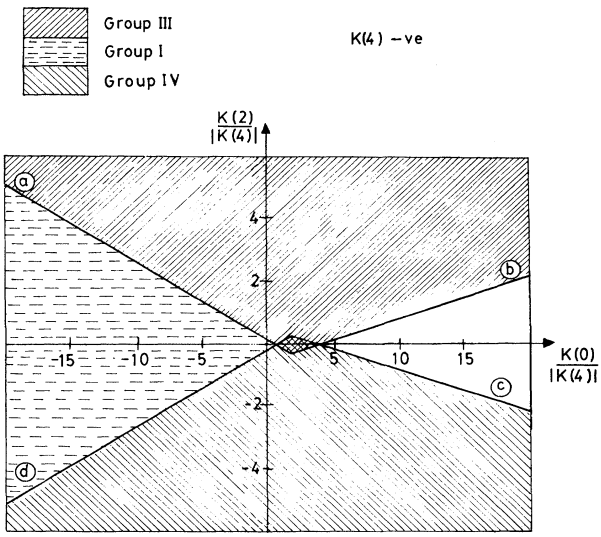

FIG. 4. The regions for the various potential minima in the $K(0)/|K(4)|$ and $K(2)/|K(4)|$ plane for a negative value of $K(4)$.

one gets potential minima along group-IV directions only.

(v) For

$$\begin{aligned} &-\frac{12}{7} < \frac{K(2)}{|K(4)|} < \frac{12}{7}\,, \\ &-\frac{8}{7} + \frac{1}{2}\frac{K(0)}{|K(4)|} < \frac{K(2)}{|K(4)|} < \frac{8}{7} - \frac{1}{2}\frac{K(0)}{|K(4)|}\,, \\ &\frac{1}{7} + \frac{1}{4}\frac{K(0)}{|K(4)|} < \frac{K(2)}{|K(4)|} < -\frac{1}{7} - \frac{1}{4}\frac{K(0)}{|K(4)|}\,, \end{aligned} \tag{15}$$

we get potential minima along group-III directions only.

The more interesting feature is that for a certain set of values of the potential parameters, we get simultaneous potential minima along two sets of orientational configurations of the impurity. These are given as follows.

(vi) For $K(4)$ positive and

$$\begin{aligned} &\frac{K(2)}{|K(4)|} > \frac{12}{7}\,, \\ &\frac{8}{7} - \frac{1}{2}\frac{K(0)}{|K(4)|} > \frac{K(2)}{|K(4)|} > -\frac{1}{7} - \frac{1}{4}\frac{K(0)}{|K(4)|}\,, \end{aligned} \tag{16}$$

we get potential minima simultaneously along group-II and -III directions.

(vii) Similarly, for $K(4)$ positive and

$$\begin{aligned} &\frac{K(2)}{|K(4)|} < -\frac{12}{7}\,, \\ &-\frac{8}{7} + \frac{1}{2}\frac{K(0)}{|K(4)|} < \frac{K(2)}{|K(4)|} < -\frac{1}{7} + \frac{1}{4}\frac{K(0)}{|K(4)|}\,, \end{aligned} \tag{17}$$

we get potential minima simultaneously along group-III and -IV directions. These are shown in Fig. 3 by overlapping shaded regions.

Similarly, the following important points could be noted for negative $K(4)$ values.

(i) No potential minima could occur along group-II directions.

(ii) For

$$\frac{5}{14}=\frac{1}{8}\frac{K(0)}{|K(4)|}<\frac{K(2)}{|K(4)|}<-\frac{5}{14}+\frac{1}{8}\frac{K(0)}{|K(4)|} \tag{18}$$

no potential minima could occur in the lattice. This has been represented by an unshaded region in Fig. 4.

(iii) For

$$-\frac{1}{7}+\frac{1}{4}\frac{K(0)}{|K(4)|}<\frac{K(2)}{|K(4)|}<\frac{1}{7}-\frac{1}{4}\frac{K(0)}{|K(4)|} \tag{19}$$

we get potential minima along group-I directions only. It may be mentioned that the group-I region does not overlap with any other region on the $K(0)/|K(4)|$ versus $K(2)/|K(4)|$ plot.

(iv) For

$$\begin{aligned}&\frac{K(2)}{|K(4)|}<-\frac{1}{7}+\frac{K(0)}{|K(4)|}\ ,\\&\frac{K(2)}{|K(4)|}<\frac{5}{14}-\frac{1}{8}\frac{K(0)}{|K(4)|}\ ,\end{aligned} \tag{20}$$

we get potential minima along the group-IV directions.

(v) For

$$\begin{aligned}&\frac{K(2)}{|K(4)|}>\frac{1}{7}-\frac{K(0)}{|K(4)|}\ ,\\&\frac{K(2)}{|K(4)|}>-\frac{5}{14}+\frac{1}{8}\frac{K(0)}{|K(4)|}\ ,\end{aligned} \tag{21}$$

we get potential minima along the group-III directions.

(vi) An interesting feature is that for a limited narrow region of the relative values of the potential parameters, we get simultaneous potential minima along the group-III and -IV directions. This is given by

$$\begin{aligned}&-\frac{1}{7}+\frac{1}{4}\frac{K(0)}{|K(4)|}>\frac{K(2)}{|K(4)|}>\frac{1}{7}-\frac{1}{4}\frac{K(0)}{|K(4)|}\ ,\\&\frac{5}{14}-\frac{1}{8}\frac{K(0)}{|K(4)|}>\frac{K(2)}{|K(4)|}>-\frac{5}{14}+\frac{1}{8}\frac{K(0)}{|K(4)|}\ .\end{aligned} \tag{22}$$

This is a very narrow region and has been suitably shown in Fig. 4 by doubly shaded region.

III. MODEL FOR THE CALCULATION OF POTENTIAL PARAMETERS $K(0)$, $K(2)$, AND $K(4)$

A. The model

The calculation of the barrier heights and the displaced position of the impurity's center of mass is based here on the multipole expansion method of the intermolecular interaction. Within the framework of this method, the reason for the center-of-mass displacement of the impurity ion can be stated as follows. The equilibrium orientational configuration of the impurity in the lattice vacancy is decided by its minimum-energy configuration. The interaction energy depends upon the distribution of the charge in the impurity ion and the ions of the host lattice. Consequently, the point of the impurity that rests at the normal lattice site in the minimum-energy orientational configuration should depend upon the distribution of charges in the impurity, the polarizability value of the impurity ion, the ions of the host crystal, the lattice parameters, etc. This point, as has been done earlier,[29] is named the center of interaction (CI) because it is this point of the impurity at which the effective crystalline field interaction acts (see Ref. 13 also). Naturally, the CI need not coincide with the center of mass (c.m.) in general, because the latter is governed by the distribution of masses in the impurity. We determine the location of the CI by assuming that the angular anisotropy of the interaction is at a minimum about this point. Such an assumption has previously been found to give a good estimate of the potential barriers hindering angular motion and off-center-of-mass displacement of the OH^- and OD^- impurities in alkali halide crystals.[6]

Let us also summarize the important points regarding the location of CI in the impurity molecule (the CI can be taken as located at the center or on the axis of symmetry). For the present case of NO_2^- impurity, it is evident that the CI will lie on the C_{2v} symmetry axis (the B axis in the notation of Ref. 22; see also Fig. 5). For an asymmetric charge distribution, CI is the point at which the angular anisotropy of the crystalline field interaction is at a minimum. The relative importance of the various types of interactions, such as electrostatic (multipole-multipole), induction, dispersion, exchange interactions, etc., which are not essentially centered at the same point, is determined by the intermolecular distances and the environ around the impurity. The CI of the asymmetric molecule (and hence the point of the impurity that rests at the normal lattice site) is therefore not a molecular constant, but depends upon the local environ of the impurity. Recently, Dreyfus[30] pointed out that for the case of the KCl:OH^- system, the tunneling splitting parameter (and hence also the off-center-of-mass displacement parameter) changes when the crystal is annealed. The position of the CI may also depend slightly upon the experimental conditions, such as temperature, pressure, state of aggregation, etc. These effects, however, will not be taken into account in the present calculations.

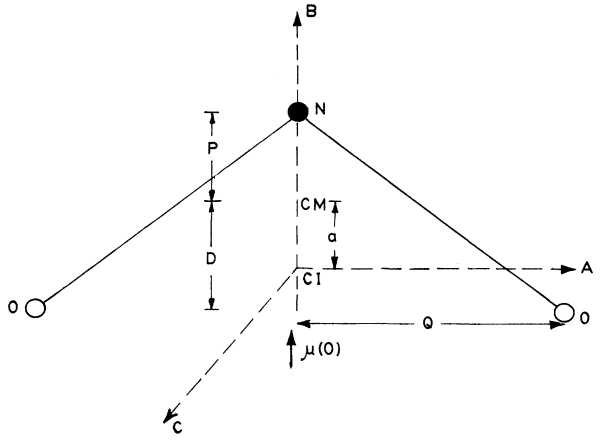

FIG. 5. Coordinates of the various atoms of the NO_2^- molecule in the molecule-fixed coordinate system.

B. Theory

The origin of the barrier for the rotation of the molecular impurities in the solid-state matrices is the angular anisotropy of the interaction between the trapped impurity and the surrounding ions of the host lattice. No impurity-impurity interaction will be considered, because most of the experimental results of interest to us are for highly dilute impurity concentrations. The main interactions are the following: (i) Electrostatic interaction (multipole-multipole), (ii) induction interaction, (iii) dispersion interaction, and (iv) exchange interaction.

The last two interactions do not enter into our formulations directly for the following reasons. The angular anisotropy in the first-order London dispersion interaction is very small[31,32] for the molecular separations of the order of 2.5–3.5 Å. The angle-dependent part of the exchange interaction is not precisely known. The only information regarding the angle-dependent part of the exchange interaction is empirical in nature and has been provided by Artman and Gordon.[33] Their empirical formula shows only a $\cos^2\theta$ dependence, which, when summed over all the neighbors of the impurity, does not give any angular anisotropy to the crystalline field. The radially dependent part of the exchange interaction does not give any contribution to the barrier, if the molecular c.m. rests at the normal lattice site. When the molecule is off centered, the exchange interaction gives a significant contribution to the $K(0)$ barrier parameter. This has been taken into account separately for the off-centered impurities [Eq. (76)].

1. Electrostatic interaction

Let XYZ represent a space-fixed coordinate system with its origin at the normal lattice vacancy, where the impurity molecule is sitting. The charges on the various lattice points of the crystal produce an electric potential at the origin. The molecular multipole moments (viz., total charge, dipole, quadrupole, and octupole moments, etc.) interact, respectively, with the electric potential, its first, second, and third gradients, etc. Thus, the interaction energy between the impurity molecule and the ions of the host lattice can be expressed as

$$V_{\text{Coul}} = e^{(S)}\phi^{(S)} - \sum_{\sigma}\mu_{\sigma}^{(S)}F_{\sigma}^{(S)} - \tfrac{1}{3}\sum_{\sigma,\tau}\theta_{\sigma\tau}^{(S)}F_{\sigma\tau}^{(S)} - \tfrac{1}{15}\sum_{\sigma,\tau,\nu}\Omega_{\sigma\tau\nu}^{(s)}F_{\sigma\tau\nu}^{(s)} - \tfrac{1}{105}\sum_{\sigma,\tau,\nu,\rho}H_{\sigma\tau\nu\rho}^{(S)}F_{\sigma\tau\nu\rho}^{(S)} , \quad (23)$$

where

$$e^{(S)} = \sum_n e_n^{(S)} ,$$

$$\mu_{\sigma}^{(S)} = \sum_n e_n^{(S)} r_{n\sigma}^{(S)} ,$$

$$\theta_{\sigma\tau}^{(S)} = \sum_n e_n^{(S)}[3r_{n\sigma}^{(S)}r_{n\tau}^{(S)} - (r_n^{(S)})^2\delta_{\sigma\tau}] ,$$

$$\Omega_{\sigma\tau\nu}^{(S)} = \sum_n e_n^{(S)}[5r_{n\sigma}^{(S)}r_{n\tau}^{(S)}r_{n\nu}^{(S)} - (r_n^{(S)})^2(r_{n\sigma}^{(S)}\delta_{\tau\nu} + r_{n\tau}^{(S)}\delta_{\sigma\nu} + r_{n\nu}^{(S)}\delta_{\sigma\tau})] ,$$

$$H_{\sigma\tau\nu\rho}^{(S)} = \sum_n e_n^{(S)}[35r_{n\sigma}^{(S)}R_{n\tau}^{(S)}r_{n\nu}^{(S)}r_{n\rho}^{(S)} - 5(r_n^{(S)})^2(r_{n\sigma}^{(S)}r_{n\tau}^{(S)}\delta_{\nu\rho} + r_{n\tau}^{(S)}r_{n\nu}^{(S)}\delta_{\sigma\rho}r_{n\nu}^{(S)}r_{n\rho}^{(S)}\delta_{\sigma T} + r_{n\rho}^{(S)}r_{n\sigma}^{(S)}\delta_{\tau\nu}r_{n\sigma}^{(S)}r_{n\nu}^{(S)}\delta_{\tau\rho} + r_{n\tau}^{(S)}r_{n\rho}^{(S)}\delta_{\sigma\nu}) + (r_n^{(S)})^4(\delta_{\sigma\tau}\delta_{\nu\tau} + \delta_{\sigma\nu}\delta_{\tau\rho} + \delta_{\sigma\rho}\delta_{\nu\tau})] ,$$

denote the electric multipole moments of the impurity molecule in the space-fixed coordinate system XYZ. $\phi_H^{(S)}$ is the electrostatic potential due to the charge on the Hth ion at the impurity site. The potential is thus given by

$$\phi^{(S)} = \sum_H \phi_H^{(S)} . \quad (24)$$

The F's in Eq. (23) denote the various gradients of the electric potential as detailed below:

$$F_{\sigma}^{(S)} = -\sum_H \nabla_{\sigma}(\phi_H^{(S)}) = \sum_H T_{\sigma}^{(H)}e^{(H)} , \quad (25)$$

$$F_{\sigma\tau}^{(S)} = -\sum_H \nabla_{\sigma}\nabla_{\tau}(\phi_H^{(S)}) = \sum_H T_{\sigma\tau}^{(H)}e^{(H)} , \quad (26)$$

$$F_{\sigma\tau\nu}^{(S)} = -\sum_H \nabla_{\sigma}\nabla_{\tau}\nabla_{\nu}(\phi_H^{(s)}) = \sum_H T_{\sigma\tau\nu}^{(H)}e^{(H)} , \quad (27)$$

$$F_{\sigma\tau\nu\rho}^{(S)} = -\sum_H \nabla_{\sigma}\nabla_{\tau}\nabla_{\nu}\nabla_{\rho}(\phi_H^{(S)}) = \sum_H T_{\sigma\tau\nu\rho}^{(H)}e^{(H)} . \quad (28)$$

The tensors are

$$T_{\sigma}^{(H)}=-\nabla_{\sigma}\left[\frac{1}{r_H^{(S)}}\right]=(r_H^{(S)})^{-2}\lambda_{\sigma}^{(H)}\ , \tag{29}$$

$$T_{\sigma\tau}^{(H)}=-\nabla_{\sigma}\nabla_{\tau}\left[\frac{1}{r_H^{(S)}}\right]=(r_H^{(S)})^{-3}(3\lambda_{\sigma}^{(H)}\lambda_{\tau}^{(H)}-\delta_{\sigma\tau})\ , \tag{30}$$

$$T_{\sigma\tau\nu}^{(H)}=-\nabla_{\sigma}\nabla_{\tau}\nabla_{\nu}\left[\frac{1}{r_H^{(S)}}\right]$$
$$=(r_H^{(S)})^{-4}[5\lambda_{\sigma}^{(H)}\lambda_{\tau}^{(H)}\lambda_{\nu}^{(H)}-(\lambda_{\sigma}^{(H)}\delta_{\tau\nu}+\lambda_{\tau}^{(H)}\delta_{\sigma\nu}+\lambda_{\nu}^{(H)}\delta_{\sigma\tau})]\ , \tag{31}$$

$$T_{\sigma\tau\nu\rho}^{(H)}=-\nabla_{\sigma}\nabla_{\tau}\nabla_{\nu}\nabla_{\rho}\left[\frac{1}{r_H^{(S)}}\right]$$
$$=-3(r_H^{(S)})^{-5}[35\lambda_{\sigma}^{(H)}\lambda_{\tau}^{(H)}\lambda_{\nu}^{(H)}\lambda_{\rho}^{(H)}-5(\lambda_{\sigma}^{(H)}\lambda_{\tau}^{(H)}\delta_{\nu\rho}+\lambda_{\tau}^{(H)}\lambda_{\nu}^{(H)}\delta_{\rho\sigma}+\lambda_{\nu}^{(H)}\lambda_{\rho}^{(H)}\delta_{\sigma\tau}+\lambda_{\rho}^{(H)}\lambda_{\sigma}^{(H)}\delta_{\tau\nu}$$
$$+\lambda_{\sigma}^{(H)}\lambda_{\nu}^{(H)}\delta_{\tau\rho}+\lambda_{\tau}^{(H)}\lambda_{\rho}^{(H)}\delta_{\sigma\nu})+(\delta_{\sigma\tau}\delta_{\nu\tau}+\delta_{\sigma\nu}\delta_{\tau\rho}+\delta_{\sigma\rho}\delta_{\nu\tau})]\ . \tag{32}$$

Here, $\lambda^{(H)}=(\lambda_x^{(H)},\lambda_y^{(H)},\lambda_z^{(H)})$ is the unit vector in the direction of the vector that connects the site of the solute molecule and that of the Hth ion of the host lattice. Now, as the lattice ions are distributed around the impurity with an octahedral symmetry, it can be shown that the first, second, and third gradients of the electric potential, viz., F_{σ}, $F_{\sigma\tau}$, and $F_{\sigma\tau\nu}$ identically vanish. The zeroth gradient, i.e., the total electric potential $\phi^{(S)}$, interacts only with the total charge of the impurity [see Eq. (23)] and gives no angular anisotropy to the interaction energy. This will, therefore, be dropped in future steps. The fourth gradient of the electric potential can be worked out explicitly. Equation (23) for the interaction energy thus reduces to

$$V_{\text{Coul}}=-\tfrac{1}{105}\sum_{\sigma,\tau,\nu,\rho}H_{\sigma\tau\nu\rho}\sum_{H}T_{\sigma\tau\nu\rho}^{(H)}\ . \tag{33}$$

Next, it can be shown that many of the 81 components of the fourth gradient tensor vanish identically because of the symmetry properties of the site and many of the remaining ones are equal. Specifically, we have the following nonvanishing components:

$$F_{XXXX}^{(S)}=F_{YYYY}^{(S)}+F_{ZZZZ}^{(S)}=-14\frac{e}{R^5}\xi_{\text{Coul}}\ , \tag{34}$$

$$F_{XXYY}^{(S)}=F_{XYYX}^{(S)}=F_{XYXY}^{(S)}=F_{YXXY}^{(S)}+F_{YXYX}^{(S)}=F_{YYXX}^{(S)}$$
$$=F_{YYZZ}^{(S)}=F_{YZZY}^{(S)}=\cdots$$
$$=F_{ZZXX}^{(S)}=\cdots=+7\frac{e}{R^5}\xi_{\text{Coul}}\ , \tag{35}$$

where ξ_{Coul} is a constant defined by

$$\xi_{\text{Coul}}=\sum_i\frac{\rho_i(\pm)n_i}{(R_i/R)^5}\ . \tag{36}$$

Here, the summation i extends over the different shells of ions surrounding the molecule, ρ_i is a certain shell summation constant, and n_i is the number of ions in the shell, whose distance from the molecular ion site is R_i, R being the nearest-neighbor separation of the lattice. The values of ρ_i, R_i, and n_i are given in Table I for the first few shells. With this, the interaction energy given in Eq. (33) becomes

$$V_{\text{Coul}}=\frac{1}{105}\left[14\frac{e}{R^5}\xi_{\text{Coul}}(H_{XXXX}+H_{YYYY}+H_{ZZZZ})\right.$$
$$\left.-42\frac{e}{R^5}\xi_{\text{Coul}}(H_{XXYY}+H_{YYZZ}+H_{ZZXX})\right]\ . \tag{37}$$

As has also been mentioned earlier, the various Cartesian components XYZ refer to the space-fixed coordinate system with its center at the molecular lattice site. Thus H_{ZZZZ} is the component of the molecular hexadecapole moment referred to the space-fixed coordinate system. Specifically, H_{ZZZZ} can be expressed as

$$H_{ZZZZ}=\tfrac{1}{8}\sum_n e_n r_n^4(35\cos^4\theta_n-30\cos^2\theta_n+3)$$
$$=\tfrac{2}{3}\sqrt{\pi}\sum_n e_n r_n^4 Y_0^4(\theta_n,\phi_n) \tag{38}$$

with similar expressions for the other components. Here, (r_n,e_n,ϕ_n) is the coordinate of the nth charge of the mol-

TABLE I. Constants of the shell summation (ρ_i and χ_i), for the first few shells surrounding the impurity, used for the calculation of the barrier parameters.

Shell No.	No. of ions in the shell	R_i/R	ρ_i	χ_i
First	6	1	1.0	1.0
Second	12	$\sqrt{2}$	−0.5	0.582
Third	8	$\sqrt{3}$	−0.889	0.444
Fourth	6	2	1.0	1.0
Fifth	24	$\sqrt{5}$	0.8	0.733
Sixth	24	$\sqrt{6}$	−1.0	0.582
Seventh	12	$\sqrt{8}$	−0.5	0.582
Eighth	30	3	−0.926	0.444

ecule in the space-fixed coordinate system. When expressions like those given in Eq. (38) for the various H's are substituted in Eq. (37), we get

$$V_{\text{Coul}}=\frac{7}{18}\frac{e\sqrt{\pi}}{R^5}\xi_{\text{Coul}} \times\sum_n e_n r_n^4\{Y_0^4(\theta_n,\phi_n) +\sqrt{\tfrac{5}{14}}[Y_4^4(\theta_n,\phi_n)+Y_{-4}^4(\theta_n,\phi_n)]\} . \tag{39}$$

Next, as the molecule could have rotational degrees of freedom in the crystal matrix, it will be better to express the interaction energy in terms of the components of the molecular hexadecapole moment referred to a coordinate system fixed inside the molecular impurity. The spherical harmonics referred to the space-fixed coordinate system can be related to the molecule-fixed coordinate system by the three Eulerian angles α, β, and γ. The transformation is given by

$$Y_0^4(\theta_n,\phi_n)=\sum_{K=-L}^{+L} D_{KM}^L(\alpha,\beta,\gamma)Y_0^4(\bar{\theta}_n,\bar{\phi}_n) . \tag{40}$$

Further, as in this particular case, the trapped molecule itself has C_{2v} symmetry, the finite components of the molecular hexadecapole moment will correspond to only $K=0,\pm2,\pm4$. When all these considerations are taken into account, we get the following expression for the electrostatic interaction of the rotating molecule in the crystal:

$$\begin{aligned}V_{\text{Coul}}=\frac{7}{18}\frac{e\sqrt{\pi}}{R^5}\xi_{\text{Coul}}\Bigg[&\left[[D_{00}^4+\sqrt{\tfrac{5}{14}}(D_{04}^4+D_{0\text{-}4}^4)]\sum_n e_n r_n^4 Y_0^4(\bar{\theta}_n,\bar{\phi}_n)\right]\\ &\times\left[[D_{20}^4+\sqrt{\tfrac{5}{14}}(D_{24}^4+D_{2\text{-}4}^4)]\sum_n e_n r_n^4 Y_0^4(\bar{\theta}_n,\bar{\phi}_n)\right]\\ &\times\left[[D_{-20}^4+\sqrt{\tfrac{5}{14}}(D_{-24}^4+D_{-2\text{-}4}^4)]\sum_n e_n r_n^4 Y_0^4(\bar{\theta}_n,\bar{\phi}_n)\right]\\ &\times\left[[D_{40}^4+\sqrt{\tfrac{5}{14}}(D_{44}^4+D_{4\text{-}4}^4)]\sum_n e_n r_n^4 Y_0^4(\bar{\theta}_n,\bar{\phi}_n)\right]\\ &\times\left[[D_{-40}^4+\sqrt{\tfrac{5}{14}}(D_{-44}^4+D_{-4\text{-}4}^4)]\sum_n e_n r_n^4 Y_0^4(\bar{\theta}_n,\bar{\phi}_n)\right]\Bigg]\cdots .\end{aligned} \tag{41}$$

When an expression of the above kind is expressed in terms of the Eulerian angles α, β, and γ, we get the following expression for the angle-dependent part of the crystalline field acting at the origin of the molecule-fixed coordinate system:

$$\begin{aligned}V_{\text{Coul}}=&K(0)[\cos^4\beta+\sin^4\beta(\sin^4\alpha+\cos^4\alpha)]\\ &+K(2)\{\cos2\gamma[(-1+8\cos^2\beta-7\cos^4\beta)+\cos4\alpha(1-\cos^4\beta)]+\sin2\gamma[\sin4\alpha(-2\cos\beta+2\cos^9\beta)]\}\\ &+K(4)\{\cos4\gamma[(1-2\cos^2\beta+\cos^4\beta)+\tfrac{1}{7}\cos4\alpha(1+6\cos^2\beta+\cos^4\beta)]+\sin4\gamma[\tfrac{4}{7}\sin4\alpha(-\cos\beta-\cos^9\beta)]\} .\end{aligned} \tag{42}$$

$K(0)$, $K(2)$, and $K(4)$ are the parameters describing the barrier-hindering angular motion of the impurity (analogous to the Devonshire K parameter for the diatomic molecules). In fact (as will be seen later), this is the general form of the crystalline field acting at the molecular site. The parameters $K(0)$, $K(2)$, and $K(4)$ can be expressed as the sum of a Coulombic, a polarization, and an exchange interaction part as

$$K(0)=K(0)_{\text{Coul}}+K(0)_{\text{ind}}+K(0)_{\text{exch}} ,$$

with similar expressions for $K(2)$ and $K(4)$. It can be easily seen from the above analysis that the Coulombic contribution to these parameters is given by

$$K(0)_{\text{Coul}}=\frac{35}{24}\frac{e}{R^5}\xi_{\text{Coul}}H(0) , \tag{43}$$

$$K(2)_{\text{Coul}}=\frac{35}{32}\frac{e}{R^5}\xi_{\text{Coul}}H(2) , \tag{44}$$

$$K(4)_{\text{Coul}}=\frac{245}{768}\frac{e}{R^5}\xi_{\text{Coul}}H(4) . \tag{45}$$

Here, $H(0)$, $H(2)$, and $H(4)$ are the components of the molecular hexadecapole moment defined by

$$H(0)=\tfrac{1}{8}\sum_n e_n r_n^4(35\cos^4\bar{\theta}_n-30\cos^2\bar{\theta}_n+3) , \tag{46}$$

$$H(2)=\tfrac{1}{6}\sum_n e_n r_n^4(7\cos^2\bar{\theta}_n-1)\sin^2\bar{\theta}_n\cos2\bar{\phi}_n , \tag{47}$$

$$H(4)=\sum_n e_n r_n^4(\sin^4\bar{\theta}_n\cos4\bar{\phi}_n) . \tag{48}$$

2. *Impurity-lattice polarization interaction*

The charge distribution in the impurity produces fields at the neighboring lattice points given by

$$F_\sigma^{(H)}=T_\sigma e^{(S)}-\sum_\tau T_{\sigma\tau}\mu_\tau^{(S)}+\tfrac{1}{3}\sum_{\tau,\nu}T_{\sigma\tau\nu}\theta_{\tau\nu}^{(S)} -\tfrac{1}{15}\sum_{\tau,\nu,\rho}T_{\sigma\tau\nu\rho}\Omega_{\tau\nu\rho}^{(S)} +\tfrac{1}{105}\sum_{\tau,\nu,\rho,\eta}T_{\sigma\tau\nu\rho\eta}T_{\sigma\tau\nu\rho\eta}H_{\tau\nu\rho\eta}^{(S)}+\cdots . \tag{49}$$

Here, the first, second, etc., terms represent, respectively, the σth component of the field produced by the impurity monopole, dipole, quadrupole, etc. at the Hth lattice site of the crystal and $F_\sigma^{(H)}$ is the total field. This field at the Hth lattice ion will cause that ion to shift from its normal lattice position and will also produce a distortion in its electron cloud. These two effects are approximately describable by a polarizability relation

$$\mu_\sigma^{(H)}=\alpha^{(H)}F_\sigma^{(H)} , \tag{50}$$

where $\mu_\sigma^{(H)}$ is the ionic plus electronic moment of the Hth lattice ion, and correspondingly $\alpha^{(H)}$ is the total polarizability in the sense described by Roberts.[34] In writing Eq. (50), we are assuming isotropic polarizabilities for the host lattice ions. The interaction energy of these induced dipoles with the charge distribution of the impurity can be written as

$$\begin{aligned} V_{\text{ind}}=&e^{(S)}\phi^{(S)'}-\sum_\sigma \mu_\sigma^{(S)}F_\sigma^{(S)'}-\tfrac{1}{3}\sum_{\sigma,\tau}\theta_{\sigma\tau}^{(S)}F_{\sigma\tau}^{(S)'} \\ &-\tfrac{1}{15}\sum_{\sigma,\tau,\nu}\Omega_{\sigma\tau\nu}^{(S)}F_{\sigma\tau\nu}^{(S)'} \\ &-\tfrac{1}{105}\sum_{\sigma,\tau,\nu,\rho}H_{\sigma\tau\nu\rho}^{(S)}F_{\sigma\tau\nu\rho}^{(S)'}\cdots , \end{aligned} \tag{51}$$

where $\phi^{(S)'}$ is the electric potential at the impurity site because of the dipole moments induced at the various lattice sites of the crystal. They can be expressed as

$$\phi^{(S)'}=\sum_H(\phi_H^{(S)'}) , \tag{52}$$

where

$$\phi_H^{(S)'}=\sum_\sigma \mu_\sigma^{(H)}T_\sigma^{(H)} \tag{53}$$

and

$$F_\tau^{(S)'}=-\sum_H\nabla_\tau(\phi_H^{(S)'})=\sum_H\sum_\sigma(-T_{\sigma\tau}^{(H)}\mu_\sigma^{(H)}) , \tag{54}$$

$$F_{\tau\nu}^{(S)'}=-\sum_H\nabla_\tau\nabla_\nu(\phi_H^{(S)'})=\sum_H\sum_\sigma(-T_{\sigma\tau\nu}^{(H)}\mu_\sigma^{(H)}) , \tag{55}$$

$$F_{\tau\nu\rho}^{(S)'}=-\sum_H\nabla_\tau\nabla_\nu\nabla_\rho(\phi_H^{(S)'})=\sum_H\sum_\sigma(-T_{\sigma\tau\nu\rho}^{(H)}\mu_\sigma^{(H)}) , \tag{56}$$

$$\begin{aligned} F_{\tau\nu\rho\eta}^{(S)'}=&-\sum_H\nabla_\tau\nabla_\nu\nabla_\rho\nabla_\eta(\phi_H^{(S)'}) \\ =&\sum_H\sum_\sigma(-T_{\sigma\tau\nu\rho\eta}^{(H)}\mu_\sigma^{(H)}) . \end{aligned} \tag{57}$$

Here, the tensors T are the same as those given in Eqs. (29)–(32) and the primes on the F's signify that these are the first, second, etc., gradients of the electric potential at the impurity site because of the induced dipole moments in the ions of the host lattice. Now, because of the fact that the various lattice ions are distributed around the impurity with an octahedral symmetry, it can be seen that the contribution to the net electric potential at the impurity comes only from the dipole moments induced in the various lattice ions because of the permanent hexadecapole moment in the molecule. Similarly, a net contribution to the first gradient of the electric potential at the impurity site comes from the dipole moments induced at the various lattice points because of the permanent octupole moment in the molecule, and so on. Realizing this, and taking full advantage of expressions (52)–(57), it can be deduced that

$$\begin{aligned} V_{\text{ind}}=&\tfrac{1}{105}\sum_{\sigma,\tau,\nu,\rho,\eta}e^{(S)}H_{\tau\nu\rho\eta}^{(S)}\sum_H\alpha^{(H)}T_\sigma T_{\sigma\tau\nu\rho\eta}-\tfrac{1}{15}\sum_{\sigma,\tau,\nu,\rho,\eta}\mu_\tau^{(S)}\Omega_{\nu\rho\eta}^{(S)}\sum_H\alpha^{(H)}T_{\sigma\tau}T_{\sigma\nu\rho\eta} \\ &+\tfrac{1}{9}\sum_{\sigma,\tau,\nu,\rho,\eta}\theta_{\tau\nu}^{(S)}\theta_{\rho\eta}^{(S)}\sum_H\alpha^{(H)}T_{\sigma\tau\nu}T_{\sigma\rho\eta} , \end{aligned} \tag{58}$$

$$V_{\text{ind}}=\sum_{\sigma,\tau,\nu,\rho,\eta}(\tfrac{1}{105}e^{(S)}H_{\tau\nu\rho\eta}^{(S)}-\tfrac{1}{15}\mu_T^{(S)}\Omega_{\nu\rho\eta}^{(S)}+\tfrac{1}{9}\theta_{\tau\nu}^{(S)}\theta_{\rho\eta}^{(S)})\left[\sum_H\alpha^{(H)}(T^2)_{\tau\nu\rho\eta}\right] . \tag{59}$$

It can be shown that many of the 81 components of the tensor $(T^2)_{\tau\nu\rho\eta}$, when summed over all the neighbors, vanish identically and many of the remaining ones are equal. Specifically, we have the following nonvanishing terms:

$$\sum_H\alpha^{(H)}(T^2)_{\tau\tau\tau\tau}=\frac{18}{R^8}\xi_{\text{ind}} , \tag{60}$$

$$\sum_H\alpha^{(H)}(T^2)_{\sigma\sigma\tau\tau}=-\frac{9}{R^8}\xi_{\text{ind}} , \tag{61}$$

where ξ_{ind} is defined as

$$\xi_{\text{ind}}=\sum_i\frac{\alpha_i\eta_i\chi_i}{(R_i/R)^8} . \tag{62}$$

Here, the summation extends over the different shells of ions surrounding the impurity molecule, χ_i is another shell summation constant (analogous to ρ_i of the previous subsection). The value of χ_i for the first few shells has also been

mentioned in Table I. With this, the induction interaction energy of Eq. (59) becomes

$$V_{\text{ind}}=\frac{18}{R^8}\xi_{\text{ind}}\left[\frac{e^{(S)}}{105}[(H_{XXXX}+H_{YYYY}+H_{ZZZZ})-3(H_{XXYY}+H_{YYZZ}+H_{ZZXX})]\right]$$
$$-\tfrac{1}{15}\langle\mu_X[\Omega_{XXX}-\tfrac{3}{2}(\Omega_{XYY}+\Omega_{XZZ})]+\mu_Y[\Omega_{YYY}-\tfrac{3}{2}(\Omega_{YXX}+\Omega_{YZZ})]+\mu_Z[\Omega_{ZZZ}-\tfrac{3}{2}(\Omega_{ZXX}+\Omega_{ZYY})]\rangle$$
$$+\tfrac{1}{9}\langle(\theta_{XX}^2+\theta_{XX}^2+\theta_{XX}^2)-(\theta_{XX}\theta_{YY}+\theta_{YY}\theta_{ZZ}+\theta_{ZZ}\theta_{XX}+2\theta_{XY}^2+2\theta_{YZ}^2+2\theta_{ZX}^2)\rangle\ . \tag{63}$$

The molecular multipole moments mentioned above are with respect to a space-fixed coordinate system with its center at the molecular lattice site. These can be expressed in a way analogous to that of Eq. (38) for H_{ZZZZ}. Next, adopting the same procedure as in the preceding subsection, i.e., transforming the various spherical harmonics from a space-fixed axes system to a molecule-fixed axes system and taking full advantage of the molecular C_{2v} symmetry, it is possible to write V_{ind} in a form similar to that of Eq. (42), with the corresponding coefficients $K(0)_{\text{ind}}$, $K(2)_{\text{ind}}$, and $K(4)_{\text{ind}}$ given by

$$K(0)_{\text{ind}}=-\frac{\xi_{\text{ind}}}{R^8}[-\tfrac{15}{8}e^{(S)}H(0)+\tfrac{15}{2}\mu(0)\Omega(0)$$
$$-\tfrac{29}{4}\theta(0)^2-\tfrac{29}{32}\theta(2)^2]\ , \tag{64}$$

$$K(2)_{\text{ind}}=-\frac{\xi_{\text{ind}}}{R^8}[-\tfrac{45}{32}e^{(S)}H(2)+\tfrac{45}{16}\mu(0)\Omega(2)$$
$$-\tfrac{29}{16}\theta(0)\theta(2)]\ , \tag{65}$$

$$K(4)_{\text{ind}}=-\frac{\xi_{\text{ind}}}{R^8}[-\tfrac{105}{256}e^{(S)}H(4)-\tfrac{203}{128}\theta(0)^2]\ . \tag{66}$$

Here, $\mu(0)$, $\Omega(0)$, $\Omega(2)$, $\theta(0)$, and $\theta(2)$ are, respectively, the components of the molecular dipole, octupole, and quadrupole moments and are defined by

$$\mu(0)=\sum_n e_n r_n\cos\bar{\theta}_n\ , \tag{67}$$

$$\theta(0)=\sum_n e_n r_n^4(3\cos^2\bar{\theta}_n-1)\ , \tag{68}$$

$$\theta(2)=\sum_n e_n r_n^4\sin^2\bar{\theta}_n\cos2\bar{\phi}_n\ , \tag{69}$$

$$\Omega(0)=\sum_n e_n r_n^4(5\cos^9\bar{\theta}_n-3\cos\bar{\theta}_n)\ , \tag{70}$$

$$\Omega(2)=\sum_n e_n r_n^9\cos\bar{\theta}_n\sin^2\bar{\theta}_n\cos2\bar{\phi}_n\ , \tag{71}$$

$$e^{(S)}=\sum_n e_n\ . \tag{72}$$

3. *Electronic polarization of the impurity*

The monopole and dipole fields produced at the impurity ion site should also polarize the latter ionically as well as electronically. The dipole moment induced at the impurity site can be written as

$$\mu_\sigma^{(S)}(\text{induced})=\sigma^{(S)}F_\sigma^{(S)}\ . \tag{73}$$

Here, $F_\sigma^{(S)}$ is the total field at the impurity site because of the monopoles and dipoles at the various lattice sites of the crystal, i.e.,

$$F_\sigma^{(S)}=\sum_H(T_\sigma^{(H)}e^{(H)}-T_{\sigma\tau}\mu_\tau^{(H)})\ . \tag{74}$$

Because of the octahedral symmetry of the crystal, this field vanishes identically. Consequently, this polarization mechanism (within the framework of our calculations) does not contribute to the anisotropy of the crystalline field.

4. *Exchange interaction*

As has also been mentioned earlier, the only information about the exchange interaction between two charge distributions is its radial-dependent part, which can be expressed as

$$V_{\text{exch}}=be^{-R/\rho}\ . \tag{75}$$

If the impurity's c.m. rests at the center of the halogen ion vacancy, the exchange interaction, when summed over the nearest-neighboring ions, shows no angular anisotropy, and as such, does not contribute to any of the barrier parameters. However, if the impurity's c.m. is displaced from the center of the halogen ion vacancy, the exchange interaction does present angular anisotropy. When this is considered in detail, it is seen that it gives a contribution to the $K(0)$ barrier parameter alone. This is obtained as

$$K(0)_{\text{exch}}=12be^{-R/\rho}\left[\frac{a}{\rho}\right]^4\ ,$$
$$K(2)_{\text{exch}}=0\ , \tag{76}$$
$$K(4)_{\text{exch}}=0\ .$$

It may be mentioned that in the present calculations, exchange interaction does not give any contribution to the $K(2)$ and $K(4)$ barrier parameters. This is due to the fact that in our model, the CI is to lie on the twofold symmetry axis of the NO_2^- impurity ion.

IV. COMPUTATION OF BARRIER PARAMETERS

For a model calculation, we shall first choose a plausible set of values for the various multipole moments of the impurity, as was also done for the constants of exchange interaction of Eq. (75). The impurity's dipole moment is known from experiment to be 0.21 D. The others are two quadrupole moment components $\theta(0)$ and and $\theta(2)$, two octupole moment components $\Omega(0)$ and $\Omega(2)$, and three

hexadecapole moment components $H(0)$, $H(2)$, and $H(4)$. This makes the total number of adjustable parameters seven apart from the constants of the exchange interaction. If one considers a point-charge point-dipole model for the impurity (see Fig. 5), then the various multipole moments can be expressed as

$$\begin{aligned}
&\mu(0)=e_N P+2e_O D\ ,\\
&\theta(0)=e_N P^2+2e_O\left[D^2-\frac{Q^2}{2}\right]\ ,\\
&\theta(2)=2e_O Q^2\ ,\\
&\Omega(0)=e_N P^3+2e_O(D^9-\tfrac{3}{2}DQ^2)\ ,\\
&\Omega(2)=2e_O DQ^2\ ,\\
&H(0)=e_N P^4+2e_O(D^4-3D^2G^2+\tfrac{3}{2}Q^4)\ ,\\
&H(2)=2e_O Q^2(D^2-\tfrac{1}{6}Q^2)\ ,\\
&H(4)=2e_O Q^4\ ,
\end{aligned} \tag{77}$$

where e_N and e_O are the charges assumed to be placed on the N and O atoms of the impurity. This makes the entire set of multipole moments expressible in terms of e_N and e_O alone part from the known molecular structural constants P, D, and Q (see Fig. 5). Earlier Sauer[5] calculated the ratios of the $K(0)$, $K(2)$, and $K(4)$ parameters by assuming $e_N=+0.07e$ and $e_O=-0.035e$. Although his attempt was more exact in nature (so far as the calculation of the energy eigenvalues of the hindered rotor was concerned), he could not obtain good agreement between the infrared results and the calculated values of the transition frequencies. This is because Sauer considered only the charge-charge interaction and neglected altogether the polarization and the exchange interactions. It has been found that these latter interactions give significant contribution to the barrier parameters. Rebane *et al.*[35] developed a model on the above considerations in which they took the charges on the impurity atoms as $e_N=-0.36e$ and $e_O=-0.32e$. We do not agree with this choice, as oxygen is more electronegative than nitrogen.[36] While in the former method of estimation, the sum of the atomic charges comes to zero and the negative electronic charge is taken to be placed at the c.m. of the nitrite ion impurity, in the latter method it sums up to $-e$ and thus all the ionic charge is taken to be distributed on the impurity atoms. As the N—O bond is only 6% ionic,[36] most of the charge must reside in the bonds. Further, both these choices do not give the value of the dipole moment in the case of KCl as is obtained experimentally.[15] We have estimated these unknown parameters (e_N and e_O) from one experimental result or the other. This should be a more plausible approach. The experimental results that we use for the purpose are the following.

(i) As has also been mentioned earlier, the exchange interaction gives a contribution only to the $K(0)$ barrier parameter, even if the impurity is off centered. There is experimental evidence of NO_2^- being on center in the KCl crystal.[15] Hence, the barrier parameters for the KCl:NO_2^- should be independent of the exchange interaction.

(ii) As the oxygen atom is more electronegative than the nitrogen atom,[36] it could be concluded that an effective positive charge resides on the nitrogen atom while a negative charge resides on the oxygen atoms.

(iii) The third experimental result that we use is that the minimum-energy orientational configuration of the impurity in the KCl:NO_2^- system is one in which the symmetry axis of the molecule lies along either of the twelve $\langle 110\rangle$ directions and the O-O axes lies along the corresponding $\langle 001\rangle$ directions. For KCl:NO_2^-, this has been conclusively proved by the electric-field and stress-field-induced dichroism experiments.[16,22] This places the KCl:NO_2^- system under group IV [Eq. (5)].

(iv) Lastly, the experimental result which is used in determining e_N and e_O is the observed dipole moment of NO_2^- in the KCl crystal, which is 0.21 D and which is attributed to the dipole moment about the c.m. This gives

$$2e_O D+e_N P=0.21\ . \tag{78}$$

Based on the above experimental results, we proceed to estimate the value of e_N and e_O as follows. According to the definition of the CI, we know that the anisotropy of angular interaction for rotations about the CI is at a minimum. From this we conclude that the barriers hindering angular motion of the impurity for its rotation about the A, B, and C axes (see Fig. 5) passing through the CI should be at a minimum. The rotation of the impurity about the B axis does not depend upon the off-center displacement parameter. On the other hand, the barrier-hindering rotation about the A and C axes does depend upon the off-center-of-mass displacement parameter. The expression for these barriers (written as V_{0A}, V_{0B}, and V_{0C}) can be obtained by simplifying Eq. (42) for rotations about the fixed axis in question. Expressions for these parameters in terms of $K(0)$, $K(2)$, and $K(4)$ for the impurity orientations, as listed in groups I–IV [Eqs. (2)–(5)], are presented in Table II for ready reference.

For group-IV directions,

$$V_{0A}=\frac{K(0)}{2}-2K(2)-\tfrac{2}{7}K(4)\ , \tag{79}$$

$$V_{0B}=-4K(2)\ , \tag{80}$$

$$V_{0C}=\frac{K(0)}{2}-2K(2)-2K(4)\ . \tag{81}$$

Hence, according to the definition of the CI, we should have

$$\left[\frac{\partial V_{0A}}{\partial x}\right]_{x=a}=0 \quad\text{and}\quad \left[\frac{\partial V_{0C}}{\partial x}\right]_{x=a}=0$$

and their second derivative should be positive. Here, a denotes off-center displacement. These two conditions give one and the same equation, viz.,

TABLE II. Crystalline field potential for rotation about different axes and corresponding librational frequencies in terms of the potential parameters V_{0A}, V'_{0A}, etc., which in turn are expressed in terms of the parameters $K(0)$, $K(2)$, and $K(4)$.

	Group I	Group II	Group III	Group IV
$V_c(A)$	$\frac{V_{0A}}{2}(1-\cos 4\psi_a)$	$\frac{V_{0A}}{2}(1-\cos 2\psi_a)+\frac{V'_{0A}}{2}(1-\cos 4\psi_a)$	$\frac{V_{0A}}{2}(1-\cos 2\psi_a)+\frac{V'_{0A}}{2}(1-\cos 4\psi_a)$	$\frac{V_{0A}}{2}(1-\cos 4\psi_a)$
V_{0A}	$-\frac{1}{2}K(0)+2K(2)-\frac{2}{7}K(4)$	$\frac{1}{2}K(0)+2K(2)-2K(4)$	$-\frac{1}{2}K(0)-2K(2)+2K(4)$	$\frac{1}{2}K(0)-2K(2)-\frac{2}{7}K(4)$
V'_{0A}	0	$-\frac{3}{8}K(0)+\frac{3}{2}K(2)-\frac{3}{14}K(4)$	$-\frac{3}{8}K(0)+\frac{3}{2}K(2)-\frac{3}{14}K(4)$	0
$V_c(B)$	$\frac{V_{0B}}{2}(1-\cos 4\psi_b)$	$\frac{V_{0B}}{2}(1-\cos 2\psi_b)+\frac{V'_{0B}}{2}(1-\cos 4\psi_b)$	$\frac{V_{0B}}{2}(1-\cos 4\psi_b)$	$\frac{V_{0B}}{2}(1-\cos 2\psi_b)+\frac{V'_{0B}}{2}(1-\cos 4\psi_b)$
V_{0B}	$-\frac{96}{7}K(4)$	$4K(2)$	$-\frac{96}{7}K(4)$	$-4K(2)$
V'_{0B}	0	$-\frac{12}{7}K(4)$	0	$-\frac{12}{7}K(4)$
$V_c(C)$	$\frac{V_{0C}}{2}(1-\cos 4\psi_c)$	$\frac{V_{0C}}{2}(1-\cos 4\psi_c)$	$\frac{V_{0C}}{2}(1-\cos 4\psi_c)+\frac{V'_{0c}}{2}(1-\cos 4\psi_c)$	$\frac{V_{0C}}{2}(1-\cos 2\psi_c)+\frac{V'_{0c}}{2}(1-\cos 4\psi_c)$
V_{0C}	$-\frac{1}{2}K(0)-2K(2)-\frac{2}{7}K(4)$	$\frac{1}{2}K(0)+2K(2)+\frac{2}{7}K(4)$	$\frac{1}{2}K(0)+2K(2)-2K(4)$	$\frac{1}{2}K(0)-2K(2)-2K(4)$
V'_{0c}	0	0	$\frac{3}{8}K(0)-\frac{3}{2}K(2)-\frac{3}{14}K(4)$	$\frac{3}{8}K(0)-\frac{3}{2}K(2)-\frac{3}{14}K(4)$
ν_a(lib)	$4(V_{0A}\tilde{A})^{1/2}$	$2[(V_{0A}+4V'_{0A})\tilde{A}]^{1/2}$	$2[(V_{0A}+4V'_{0A})\tilde{A}]^{1/2}$	$4(V_{0A}\tilde{A})^{1/2}$
ν_b(lib)	$4(V_{0B}\tilde{B})^{1/2}$	$2[(V_{0B}+4V'_{0B})\tilde{B}]^{1/2}$	$4(V_{0B}\tilde{B})$	$2[(V_{0B}+4V'_{0B})\tilde{B}]^{1/2}$
ν_c(lib)	$4(V_{0C}\tilde{C})^{1/2}$	$4(V_{0C}\tilde{C})^{1/2}$	$2[(V_{0C}+4V'_{0C})\tilde{C}]^{1/2}$	$2[(V_{0C}+4V'_{0C})\tilde{C}]^{1/2}$

$$\left[\frac{35}{24}\frac{\xi_{\text{Coul}}e}{R^5}[2\Omega(0)-3\Omega(2)]+\frac{13}{8}\frac{\xi_{\text{ind}}}{R^8}\mu(0)[2\theta(0)-\theta(2)]\right]$$
$$+\left[\frac{35}{8}\frac{\xi_{\text{Coul}}e}{R^5}[2\theta(0)-\theta(2)]+\frac{13}{8}\frac{\xi_{\text{ind}}}{R^8}\{-e[2\theta(0)-\theta(2)]+4\mu(0)^4\}\right]a$$
$$+\left[\frac{35}{4}\frac{\xi_{\text{Coul}}e}{R^5}\mu(0)+\frac{13}{4}\frac{\xi_{\text{ind}}}{R^8}[-3e\mu(0)]\right]a^2+\left[-\frac{35}{12}\frac{\xi_{\text{Coul}}e^2}{R^5}+\frac{39}{12}\frac{\xi_{\text{ind}}}{R^8}e^2+\frac{b}{3\rho^4}e^{-R/\rho}\right]a^3=0\ . \quad (82)$$

In deducing the above expression, use has been made of the fact that the parameters P,D of the impurity as shown in Fig. 5 change to $P+a$ and $D-a$ due to off-center displacement. Substituting these in Eq. (77) we obtain equations relating the multipole moments of the charge distribution about axes passing through its CI to those passing through its c.m. as

$$\mu(0)_{\text{CI}}=\mu(0)_{\text{c.m.}}+a(-e)\ ,$$
$$\theta(0)_{\text{CI}}=\mu(0)_{\text{c.m.}}+2a\mu(0)_{\text{c.m.}}+a^2(-e)\ ,$$
$$\theta(2)_{\text{CI}}=\theta(2)_{\text{c.m.}}\ ,$$
$$\Omega(0)_{\text{CI}}=\Omega(0)_{\text{c.m.}}+3a\theta(0)_{\text{c.m.}}+3a^2\mu(0)_{\text{c.m.}}+a^3(-e)\ ,$$
$$\Omega(2)_{\text{CI}}=\Omega(2)_{\text{c.m.}}+a\theta(2)_{\text{c.m.}}\ , \quad (83)$$
$$H(0)_{\text{CI}}=H(0)_{\text{c.m.}}+4a\Omega(0)_{\text{c.m.}}+6a^2\theta(0)_{\text{c.m.}}+4a^3\mu(0)_{\text{c.m.}}+a^4(-e)\ ,$$
$$H(2)_{\text{CI}}=H(2)_{\text{c.m.}}+2a\Omega(2)_{\text{c.m.}}+a^2\theta(2)_{\text{c.m.}}\ ,$$
$$H(4)_{\text{CI}}=H(4)_{\text{c.m.}}\ .$$

Equations (82) can thus be used for determining the values of a for the present systems of interest. Now, the experimental observation that for the KCl:NO_2^- system $a=0$, gives

$$\left[\frac{35}{24}\frac{\xi_{\text{Coul}}e}{R^5}[2\Omega(0)-3\Omega(2)]+\frac{13}{8}\frac{\xi_{\text{ind}}}{R^8}\mu(0)[2\theta(0)-\theta(2)]\right]=0\ . \quad (84)$$

TABLE III. Impurity constants used in the calculations.

$\tilde{A}$ (cm^{-1})	4.22[a]
$\tilde{B}$ (cm^{-1})	0.45[a]
$\tilde{C}$ (cm^{-1})	0.43[a]
$\mu_{\text{intrinsic}}$(D)	0.21[b]
N—O, (Å)	1.24[a]
∢O—N—O (deg)	118[a]
e_N	$0.059e$[c]
e_O	$-0.045e$[c]
b (10^{-9} erg)	3.8[c]
ρ (Å)	0.345[c]

[a]Rotational constants about the three axes A, B, and C.
[b]From Ref. 16.
[c]Obtained from known experimental results (see text).

When the various multipole moments in the above equation are expressed in terms of e_N and e_O and the molecular structural parameters as detailed in Eq. (77), we get a relation between e_N and e_O and other known parameters of the system. This expression, when solved with the help of Eq. (78), gives an estimate of the charges on N and O atoms of the impurity. In our case, we have calculated it to be $e_N=0.059e$ and $e_O=-0.045e$. With these values of the fractional charges on the nitrogen and the oxygen atoms and the known structural parameters of the molecule (see Table III) the various components of its multipole moment are evaluated. These are given in Table IV. The rest of the charge of the impurity, viz.,

$$e_C=-e+e_N+e_O \quad (85)$$

can be attributed as being placed at the center of mass of the impurity molecule.

The barrier parameters can now be easily calculated for the KCl:NO_2^- impurity in other crystals; the value of the off-center-of-mass displacement parameter a is first calculated as usual from Eqs. (43)–(45), (64)–(66), and (76). The calculated values of these parameters for systems of interest are given in Table V.

V. RESULT AND DISCUSSION

A. Impurity orientations

The sign and the relative magnitudes of the barrier parameters allow us to predict the minimum-energy orientational configuration of the impurity. As $K(4)$ is negative for the systems of interest here, we refer to Fig. 4 in this work for discussion. The relative values of the barrier parameters, i.e., $(K(0)/|K(4)|, K(2)/|K(4)|)$ in the case of the KCl:NO_2^- and the KBr:NO_2^- systems, are

TABLE IV. Computed values of multipole moments of NO_2^- about the center of mass used for the calculation of the barrier parameters.

$\mu(0)_{\text{c.m.}}$ (D)	+0.21
$\theta(0)_{\text{c.m.}}$ (D Å)	+0.284
$\theta(2)_{\text{c.m.}}$ (D Å)	−0.488
$\Omega(0)_{\text{c.m.}}$ (D $Å^2$)	−0.114
$\Omega(2)_{\text{c.m.}}$ (D $Å^2$)	+0.095
$H(0)_{\text{c.m.}}$ (D $Å^3$)	−0.141
$H(2)_{\text{c.m.}}$ (D $Å^3$)	−0.057
$H(4)_{\text{c.m.}}$ (D $Å^3$)	−0.552

TABLE V. Calculated values of the barrier hindering angular motion parameters and off-center-of-mass displacement parameter for the NO_2^- impurity in different crystal lattices.

	KCl:NO_2^-	KBr:NO_2^-	KI:NO_2^-
a (Å)	0	−0.08	−0.15
$K(0)$ (cm^{-1})	−88.12	2.00	188.14
$K(2)$ (cm^{-1})	−33.65	−17.82	−0.25
$K(4)$ (cm^{-1})	−80.86	−69.10	−47.37
V_{0A} (cm^{-1})	46.34	56.39	118.11
V_{0B} (cm^{-1})	134.60	71.29	1.02
V'_{0B} (cm^{-1})	138.61	118.46	81.20
V_{0C} (cm^{-1})	184.96	174.85	189.32
V'_{0C} (cm^{-1})	34.75	42.29	81.09

(−1.10, −0.42) and (0.03, −0.26), respectively, which places these impurity systems in group IV, for which the symmetry axis of the molecule lies along either of the twelve ⟨110⟩ directions and the O—O bond parallel to the corresponding ⟨001⟩ directions. For the KCl:NO_2^- system, this has been conclusively proved by the electric- and stress-field dichroism experiments.[1,16] Interestingly, the relative values of the barrier parameters in the case of the KI:NO_2^- system are (3.94, −0.005), which places this system in the doubly shaded region of Fig. 4, predicting a simultaneous occurrence of potential minima along group-III and -IV directions. This will have an important bearing on the infrared results, which are taken up in further discussions.

B. Off-center-of-mass displacement

In KCl, the nitrite ion sits at the normal lattice site, as concluded experimentally by Sack and Moriarty.[15] We have used this result to obtain the values of the fractional charges e_N and e_O. Also, in the case of the KI:NO_2^- system, Sack and Moriarty measured its dipole moment as 0.97 D. This large value of the dipole moment is due to a large off-center-of-mass displacement of NO_2^- from the normal lattice site in the KI crystal. Narayanamurty[16] explained this large off-center-of-mass displacement by assuming that the nearest I^- ion in KI is highly polarized and attracts N towards itself. But such a displacement will give the dipole moment opposite to the intrinsic dipole moment, and must be as large as 0.25 Å. Our calculations predict a displacement by 0.15 Å of the impurity c.m. along the ⟨110⟩ direction in the KI:NO_2^- system. This gives an additional dipole moment of 0.72 D to the molecule in the lattice. Also, the sign of the displacement parameter a shows that the direction of the displacement dipole moment is the same as that of the intrinsic dipole moment of the impurity ion. Thus the resultant dipole moment of the impurity ion in the KI lattice becomes (0.72+0.21)=0.93 D. This can be taken as a fairly nice agreement between the calculations based on the model in this work and the experimental results.[15]

Our calculations for the KBr:NO_2^- system shows that in this case also, the impurity ion is displaced by about 0.08 Å from the normal lattice site. The value of the displacement dipole moment in this case becomes 0.38 D. The resultant dipole moment of the impurity in this system becomes (0.38+0.21)=0.59 D. Experiments determining the resultant dipole moment of this impurity in KBr have not been performed. Infrared and other spectroscopic studies do not conclusively predict the off-center configuration for this system. However, there are speculations[1,16] that the NO_2^- ion sits at a slightly off-centered position in the KBr lattice. Our discussion for the infrared data also supports this point of view.

C. Infrared spectra

With the calculated values of the barrier parameters and the form of the detailed crystalline field, it is now possible to extend a reasonable explanation for the infrared studies also. The infrared spectra of these systems consist of the ν_1, ν_2, and ν_3 (see Fig. 1 of Ref. 16) internal vibrational lines, which are accompanied by the rotational fine structure. Moreover, as has been suggested also by Narayanamurty *et al.*,[16] we can treat the rotations about the three axes of inertia independently. Under such an assumption, the ν_1 and ν_2 vibrations are expected to be sensitive to the rotations about the A and C axes and not to that about the B axis. Similarly, the ν_3 vibration will be sensitive to the rotations about the B and C axes and not to that about the A axis. Let us consider these rotations separately.

For the rotation about the A axis, the crystalline field potential [see Eq. (42)] reduces to

$$V_C=\frac{V_{0A}}{2}(1-\cos 4\psi_a)\ , \tag{86}$$

where

$$V_{0A}=\frac{K(0)}{2}-2K(2)-\tfrac{2}{7}K(4)\ . \tag{87}$$

This form of the potential [Eq. (86)] is the same as that proposed by Evans and Fitchen[22] or Avarmaa and Rebane.[17] However, it is different from the one used by Narayanamurty *et al.*[16]

For the rotation about the C axis, the plane consisting of the molecule does not change and the molecule rotates about an axis perpendicular to its plane. For this rotation the crystalline field reduces to

$$V_C=\frac{V_{0C}}{2}(1-\cos 2\psi_C)+\frac{V'_{0C}}{2}(1-\cos 4\psi_c)\ , \tag{88}$$

where

$$V_{0C}=\frac{K(0)}{2}-2K(2)-2K(4)\ , \tag{89}$$

$$V'_{0C}=-\tfrac{3}{8}K(0)-\tfrac{3}{2}K(2)-\tfrac{3}{14}K(4)\ . \tag{90}$$

The values of the parameters V_{0C} and V'_{0C} have been mentioned in Table II for the systems of interest.

For rotation about the B axis, the crystalline field reduces to

$$V_C=\frac{V_{0B}}{2}(1-\cos 2\psi_b)+\frac{V'_{0B}}{2}(1-\cos 4\psi_b)\ , \tag{91}$$

where

$$V_{0B} = -4K(2) , \tag{92}$$

$$V'_{0B} = -\tfrac{12}{7}K(4) . \tag{93}$$

If the barrier parameters V_{0B}, V'_{0B}, V_{0C}, V'_{0C}, etc., are high enough, the molecule will not be able to perform free or hindered rotation, but will at best librate about its mean equilibrium orientation. These librational frequencies can be worked out very well in terms of barrier parameters V_{0A}, V'_{0A}, etc., and the rotational constants $\tilde{A}$, etc., and are summarized in Table II for ready reference. The infrared results for the impurity systems of our interest are obtained as follows.

1. The KCl:NO_2^- system

For this system, the value of the off-center displacement parameter a is zero. Hence, it is reasonable to think that in KCl, the various angular motions are taking place about the principal axes passing through the center of mass. Figure 6 represents the energy-level diagram for the NO_2^- molecule in the KCl for the simultaneous rotation of the molecule about the A and C axes. For rotation about the C axis, it should be mentioned that this rotation is highly hindered. This is because of the large values of barrier parameters V_{0C} and V'_{0C} and the small value of the corresponding rotational constant. Thus, about the C axis the molecule can only librate in either of the two equivalent well minima. The librational frequency is given by

$$\nu_c(\text{lib}) = 2[(V_{0C} + 4V'_{0C})\tilde{C}]^{1/2} , \tag{94}$$

which turns out to be 23.6 cm^{-1} for this case. Each librational level will be twofold degenerate, corresponding to the localization of the molecule in either of the two wells. However, the molecule can tunnel quantum mechanically into the other well. This splits the individual librational level. The tunneling splitting can be calculated with the help of the barrier parameters calculated in this work (Table V) and the standard tables of Mathieu's eigenvalues.[37] The tunneling splitting parameter for the present case turns out to be 0.0013 cm^{-1}. This is too small to be resolved in the infrared spectra or to give any appreciable width to the individual vibrational-rotation lines corresponding to the rotation of the molecule about the A axis. Thus, we come to the conclusion that the level structure of the impurity for the explanation of the ν_1 and ν_2 bands will be as follows. The ground vibrational level will have torsional oscillator structure corresponding to the torsional motion about the C axis. Then the ground and the first, etc., excited torsional levels corresponding to the libration about the C axis will be further split into the A_1, E, B_1, and B_2 structure, because of the simultaneous rotation of the molecule about the A axis.

It is reasonable to assume that the structure and other parameters of the molecule remain more or less the same in the first excited vibrational state also. Hence the same librational-rotational level structure will be seen with the first excited vibrational level also. Figure 6 comprehensively illustrates this. Table VI presents the calculated frequencies of the various allowed transitions and compares them to the experimental values. Table VII presents the calculated relative intensities of these lines at 2 and 15 K and compares them to the experimental results. From Tables VI and VII, it can be seen that the calculated values of the line frequencies, their relative intensities at one temperature, and the variation of these intensities with temperature agree very well with the experiments.

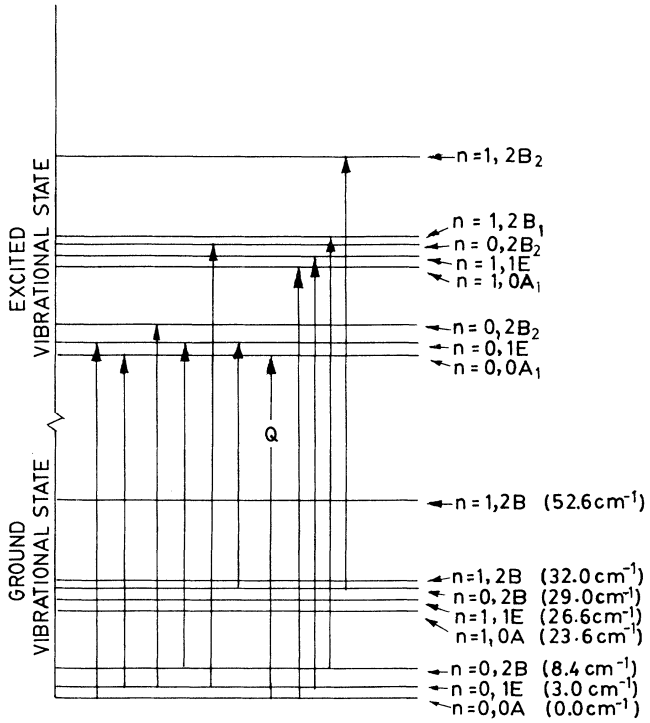

FIG. 6. Level structure for the ground and first excited vibrational state of the NO_2^- impurity in the KCl lattice corresponding to the simultaneous rotation about the A axis and libration about the C axis. These have been obtained with values of V_{0A}, V_{0C}, and V'_{0C} as mentioned in Table V. Hence, n designates the harmonic-oscillator quantum number corresponding to the libration about the C axis and A_1, E, B_1, and B_2 are the designations of the level structure corresponding to the rotation of the molecule about the A axis. The arrows represent the allowed transitions, thermally populated at the temperature of our interest.

We now come to the discussion of the fine structure observed with the ν_3 band. The fine structure in this case is to be explained in terms of the rotation of the molecule about the B and C axes. From the calculated values of the barrier parameters (Table V), the librational frequency about the C axis turns out to be 23.6 cm^{-1}. A sum satellite at about 24 cm^{-1} from the band center has indeed been observed. The corresponding difference satellite will naturally be too weak to be observed. The sum and the difference satellites at 4–5 cm^{-1} from the band center have been interpreted by Narayanamurty *et al.*[16] to arise because of the librational motion of the impurity about the B axis. Librational frequency about the B axis is given by

TABLE VI. Assignment of the transitions associated with the ν_1 and ν_2 vibrations in the KCl host lattice.

Transition[a]	Calculated frequencies ν_1	Calculated frequencies ν_2	Observed frequencies[b] ν_1	Observed frequencies[b] ν_2
$0,0A_1-0,1E$	1330	806	1329	805
$0,1E-0,2B_1$	1332.4	808.4	1332	809
$0,1E-0,0A_1$	1324	802	1325	801
$0,2B_1-0,1E$	1321.6	797.6	1322	797
$0,1E-0,2B_2$	1353	829		
$0,2B_2-0,1E$	1301	777		
$0,0A_1-1,0A_1$ $0,1E-1,1E$ $0,2B_1-1,2B_1$ $0,2B_2-1,2B_2$	1350.6	826.6	1349	817
$0,0A_1-0,0A_1$ etc. [$Q(0)$ branch]	1327	803	1327	803

[a]For designation of the levels, see the caption to Fig. 6 and the text.
[b]Reference 16.

$$\nu_b(\text{lib})=2[(V_{0B}+4V'_{0B})\tilde{B}]^{1/2} . \quad (95)$$

From the calculated values of the barrier parameters, the librational frequency about the B axis in our case turns out to be 35.2 cm^{-1}. Hence, in light of the present calculations, we can say that the sum and the difference satellites at 4–5-cm^{-1} separation cannot arise because of the librational motion of the molecule about the B axis. At the present moment we are not in a position to present an alternative explanation to these absorptions other than to say that, probably, in the solid state some of the forbidden transitions might become allowed. In fact, our inability to extend an explanation for this might be because of the fact that we are treating the rotations of the impurity about the three axes independently. A better approach demands the solution of the rotational levels of an asymmetric top molecule of C_{2v} symmetry in an octahedral field. This was attempted by Sauer,[5] but the calculation of the ratios of the barrier parameters was too simple and approximate to provide a detailed explanation of the experimental data. Work in this direction is in progress.

TABLE VII. Calculated and observed relative intensities of the various lines in the rotational fine structure of ν_1 and ν_2 vibrations of the KCl:NO_2^- system.

Transition (cm^{-1})	Calculated relative intensity[a] 2 K	Calculated relative intensity[a] 15 K	Observed relative intensity[b] 2 K	Observed relative intensity[b] 15 K
805	89	46	85	57
801	10	34	14	37
809	10	34	17	34
797	1	20	1	7

[a]In arbitrary units.
[b]From Ref. 16.

2. *The KBr:NO_2^- system*

For this system, the experimental results regarding the rotational fine structure of the vibrational lines are similar to those observed in the KCl:NO_2^- case. The difference is that the fine-structure lines are more closely spaced. This is qualitatively consistent with our calculations, where we get larger values of the barrier parameters and smaller rotational constants. We have considered the CI as the point about which the angular anisotropy of the interaction is at a minimum. Obviously, a molecule left to itself in the lattice will perform various angular motions about the CI and not the c.m. This will make the effective rotational constants for the impurity's motion about the A and C axes smaller and the corresponding fine-structure lines are more closely spaced. Figure 7 represents the energy-level diagram of the KBr:NO_2^- system for the simultaneous rotation about the A and C axes. Quantitatively, Table VIII gives the calculated positions of the line frequencies as obtained from the barrier parameters given in Table V. It can be seen that the sum and the difference satellites at about 1 cm^{-1} observed with the ν_1 and ν_2 lines are well explained. The transition corresponding to the librational motion of the molecule about the C axis has been obtained to occur at 822.8 cm^{-1}, whereas that experimentally observed is at 815 cm^{-1}. Moreover, the other lines at 808, 809.5, and 811 cm^{-1} are not accounted for in terms of the present calculations. Quite likely, they may be associated with the combined translational-librational motion of the impurity in the lattice vacancy and may owe their explanation to an approach similar to that of Bilz *et al.*,[38] with the inclusion of a possible rotation-translation coupling (see also the discussion of the KI:NO_2^- system).

3. *The KI:NO_2^- system*

Many experiments have been performed for this system. Narayanamurti *et al.*[16] summarized the available

TABLE VIII. Assignment of the transitions associated with the ν_1 and ν_2 vibrations in the KBr host-lattice.

Transitions[a]	Calculated frequencies ν_1	Calculated frequencies ν_2	Observed frequencies[b] ν_1	Observed frequencies[b] ν_2
$0,0A_1-0,1E$	1320.1	799.6	1320	799.5
$0,1E-0,2B_1$	1320.2	799.7		
$0,1E-0,0A_1$	1317.9	797.4	1318	797.5
$0,2B_1-0,1E$	1317.8	797.3		
$0,1E-0,2B_2$	1377.0	856.5		
$0,2B_2-0,1E$	11261	740.5		
$0,0A_1-1,0A_1$				
$0,1E-1,1E$	1343.3	822.8		815
$0,2B_1-1,2B_1$				
$0,2B_2-1,2B_2$				
$0,0A_1-0,0A_1$ etc. [$Q(0)$ branch]	1319	798.5	1319	798.5

[a]For designation of the levels, see the caption to Fig. 7 and the text.
[b]Reference 16.

experimental results for this system (see Table III of Ref. 16). A possible explanation of the various absorption peaks presented by Bilz *et al.*[38] was shown to be unsuitable in Ref. 16, as it was considered an unreasonably small value of the O—N—O bond angle. Narayanamurti *et al.*[16] presented an alternative explanation in terms of libration of the molecule about the A and C axes, to which the free rotation about the B axis is coupled. In their explanation, they concluded that the barriers hindering different angular motion in this case should be large compared to the corresponding barriers in the case of $KCl:NO_2^-$ system. Our calculations support this point of view. The large value of the off-center displacement decreases the rotational constant and, as a result, the rotational fine structure will not be observed. However, in view of the various limitations of our model for the calculation of the barriers, it may not be worthwhile to attempt a detailed point-to-point explanation of the infrared work. As all the barrier heights are large in this case, the rotation about all three axes will be remarkably hindered. As such, three librational lines are expected. However, Narayanamurti *et al.*[16] have observed altogether six lines at 53, 63, 71, 79, 137, and 206 cm^{-1}. Interestingly, our calculations put $KI:NO_2^-$ in the category in which the impurity can have two sets of orientations simultaneously—along groups III and IV. It is speculated that these six lines are due to the libration of the impurity about the three axes in the above-mentioned two orientations. Our calculations give the librational frequencies about A, B, and C axes as 82.7, 24.2, and 28.7 cm^{-1} for the group-IV orientation and as 46.4, 68.4, and 28.2 cm^{-1} for the group-III orientation. It can be assumed that the lines observed at 53, 71, and 79 cm^{-1} correspond to 46.4, 68.4, and 82.7 cm^{-1} of our calculations. At the present moment, we are not in a position to say anything more than this for the $KI:NO_2^-$ system. A more systematic approach will be to consider the combined translational-rotational or librational motion of the molecule in the field of octahedral symmetry. As experiments (and also our calculations) predict that the NO_2^- molecule sits off centered in this lattice, and that the various rotations are taking place about the CI and not about the c.m., it may be essential to consider a possible rotation or libration-translation coupling of the molecular motion. This kind of a coupling has been found to explain most of the experimental results in the HCl:Ar, etc., type of systems at 4.2 K.[39–41] Quite likely, it is possible that an approach similar to that of Bilz *et al.*[38] and which also incorporates a possible rotation-translation

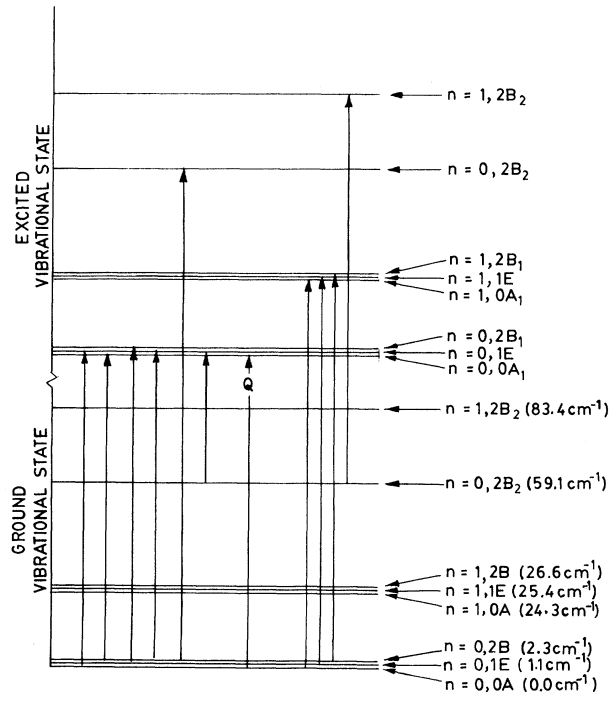

FIG. 7. Same as Fig. 6, but for the NO_2^- impurity in the KBr lattice.

coupling may explain all the experimental observations simultaneously. Work in this direction is in progress.

VI. SUMMARY

Theoretical investigation of the model potential leads to the conclusion that the NO_2^- impurity can have four types of orientations in the alkali halide lattices. Interestingly, for some sets of relative values of the barrier parameters, the impurity can orient simultaneously in two crystallographic directions.

From the results obtained on the basis of the microscopic model developed in Sec. III and the discussion that follows, it is concluded that in KCl most of the features of the infrared spectra are explained in terms of the rotational motion of the molecule about different principal axes of inertia. The translational motion of the impurity does not provide any resonant or localized mode absorption in the frequency range of our interest. Also, the translational motion does not influence (or couple) to the rotational motion of the molecule about different axes of inertia. In KI, the picture is different. Here the impurity is considerably off centered and performs different rotations about the axes passing through the center of interaction. In such a situation, the rotational and the translational modes of the molecule get coupled. This coupling should in some way be proportional to the off-center displacement parameter a. This gives rise to a complicated infrared spectra for this system. In KBr:NO_2^-, the impurity is again off centered but not to the extent that it was in KI:NO_2^-. Hence, in this case also, the explanation of things in terms of the rotational motion alone does not meet with as great a success as in the KCl:NO_2^- case. We believe that our calculated values of the barrier parameters, etc., are significant and what is needed to be done now is to build a theory that considers the coupled rotation translation of the molecule in the field of octahedral symmetry.

ACKNOWLEDGMENTS

We are thankful to Dr. V. K. Agrawal for helpful discussions. Thanks are also due to the Council for Scientific and Industrial Research (India) for financial assistance.

[1]V. Narayanamurti and R. O. Pohl, Rev. Mod. Phys. **42**, 201 (1970).
[2]F. Bridges, Crit. Rev. Solid State Sci. **5**, 1 (1975).
[3]A. F. Devonshire, Proc. R. Soc. A **153**, 601 (1936).
[4]M. E. Bauer and W. R. Salzman, Phys. Rev. **151**, 710 (1966).
[5]P. Sauer, Z. Phys. **194**, 360 (1966).
[6]M. Gomez, S. P. Bowen, and J. A. Krumhansl, Phys. Rev. **153**, 1009 (1967).
[7]H. B. Shore, Phys. Rev. **151**, 570 (1966).
[8]S. C. Jain and V. K. Tewari, J. Phys. C **6**, 1999 (1973).
[9]G. K. Pandey, K. L. Pandey, M. Massey, and Raj Kumar, Phys. Rev. B **34**, 1277 (1986).
[10]B. G. Dick, Phys. Status Solidi B **141**, 61 (1987).
[11]G. K. Pandey and D. K. Shukla, Phys. Rev. B **4**, 4598 (1971).
[12]G. K. Pandey and D. K. Shukla, Phys. Rev. B **4**, 2757 (1971).
[13]G. K. Pandey and D. K. Shukla, Phys. Rev. B **3**, 4391 (1971).
[14]W. N. Lawless, J. Phys. Chem. Solids **28**, 1755 (1967).
[15]H. S. Sack and M. C. Moriarty, Solid State Commun. **3**, 93 (1965).
[16]V. Narayanamurti, W. D. Seward, and R. O. Pohl, Phys. Rev. **148**, 481 (1966).
[17]R. Avarmaa and L. Rebane, Phys. Status Solidi **35**, 107 (1969).
[18]T. Timusk and W. Staude, Phys. Rev. Lett. **13**, 373 (1964).
[19]A. J. Sievers and C. Lytle, Phys. Rev. Lett. **14**, 271 (1965).
[20]K. F. Renk, Phys. Lett. **14**, 281 (1965).
[21]I. W. Shepherd, A. R. Evans, and D. B. Fitchen, Phys. Lett. **27A**, 171 (1968).
[22]A. R. Evans and D. B. Fitchen, Phys. Rev. B **2**, 1074 (1970).
[23]I. W. Shepherd and D. B. Fitchen (unpublished).
[24]K. K. Rebane, L. A. Rebane, A. A. Gorokhovski, and T. J. Haldre, Adv. Raman Spectrosc. **1**, 379 (1972).
[25]T. Haldre, L. Rebane, O. Sild, and F. Jarvekulg, Eesti NSV Tead. Acad. Toim., Fuus. Mat. **24**, 417 (1975).
[26]T. J. Haldre, L. A. Rebane, A. V. Liapzev, and A. A. Kiselev, Phys. Status Solidi B **70**, 359 (1975).
[27]L. A. Rebane, G. S. Zavt, and K. E. Haller, Phys. Status Solidi B **80**, 399 (1977).
[28]W. H. Flygare, J. Chem. Phys. **39**, 2263 (1963).
[29]H. Friedman and S. Kimel, J. Chem. Phys. **43**, 3925 (1963).
[30]R. W. Dreyfus, Solid State Commun. **7**, 827 (1969).
[31]J. O. Hirschfelder, C. F. Curtis, and R. B. Bird, *Molecular Theory of Gases and Liquids* (Wiley, New York, 1954).
[32]S. Kielich, Acta Phys. Polon. **22**, 65 (1962).
[33]J. O. Artmann and G. P. Gordon, Phys. Rev. **96**, 1237 (1954).
[34]S. Roberts, Phys. Rev. **81**, 865 (1951).
[35]L. A. Rebane, G. S. Zavt, and K. E. Haller, Phys. Status Solidi B **81**, 57 (1977).
[36]L. Pauling, *Nature of Chemical Bonds,* 3rd ed. (Cornell University Press, New York, 1960).
[37]*Tables of Mathieu Functions* (Columbia University Press, New York, 1951).
[38]H. Bilz, K. F. Renk, and K. H. Timmesfield, Solid State Commun. **3**, 223 (1965).
[39]H. Friedmann and S. Kimel, J. Chem. Phys. **43**, 3925 (1965).
[40]G. K. Pandey and S. Chandra, J. Chem. Phys. **49**, 4369 (1966).
[41]G. Turrell, *Infrared and Raman Spectra of Crystals* (Academic, New York, 1972).